Alinteri J. of Agr. Sci. (2021) 36(1): 420-432
e-ISSN: 2587-2249
info@alinteridergisi.com

http://dergipark.gov.tr/alinterizbd
http://www.alinteridergisi.com/
DOI:10.47059/alinteri/V36I1/AJAS21063

RESEARCH ARTICLE

Electron Swarm Parameters and Dielectric Properties of the Superconducting Binary Mixtures of He-H_2

Mohammad M. Othman[1*] • Sherzad A. Taha[2] • Saeed O. Ibrahim[3]

[1*]*Department of Physics, College of Education, Salahaddin University, Erbil, Kurdistan Region, Iraq.*
E-mail: muhamad.othman@su.edu.krd

[2]*Department of Physics, College of Education, Salahaddin University, Erbil, Kurdistan Region, Iraq.*

[3]*Department of Physics, College of Education, Salahaddin University, Erbil, Kurdistan Region, Iraq.*

A R T I C L E I N F O

Article History:
Received: 24.03.2021
Accepted: 25.04.2021
Available Online: 21.06.2021

Keywords:
Electron-energy Distribution Function
Boltzmann Equation
Swarm Parameters
Dielectric Strength
Dielectric Breakdown

A B S T R A C T

In this study, the electron energy distribution function EEDF, the electron swarm parameters, the effective ionization coefficients, and the critical field strength (dielectric strength) in binary He-H2 gas mixture which used as cryogenic for high-temperature superconducting power application, are evaluated by using two-term approximation of the Boltzmann equation over the range of E/N (the electric field to gas density) from 1 to 100 Td (1 Td=10^{-17} Vcm2) at temperature 77 K and pressure 2MPa, taking into account elastic and inelastic cross-section. Using the calculated EEDF, the electron swarm parameters (electron drift velocity, mean electron energy, diffusion coefficient, electron mobility, ionization and attachment coefficient) are calculated. At low reduced electric field E/N, the EEDF close Maxwellian distribution, at high E/N, due to vibrational excitation of H2 the calculated distribution function is non-Maxwellian. Besides, in the He-H2 mixture, it is found that increasing small amount of H2 enhances to shift the tail of EEDF to the lower energy region, the reduced ionization coefficient α/N. reduced effective ionization coefficient (α-η)/N) decreases, while, reduced attachment coefficient η/N, reduced critical electric field strength (E/N)crt. and critical electric field Ecrt. Increases, because of hydrogen's large ionization cross-sections. The dielectric strength of 5% H2 in mixture is in good agreement with experimental values, it is found that dielectric strength depend on pressure and temperature. The electron swarm parameters in pure gaseous helium (He) and hydrogen (H_2), in satisfying agreement with previous available theoretical and experimental values. The validity of the calculated values has been confirmed by two-term approximation of the Boltzmann equation analysis.

Please cite this paper as follows:

Othman, M.M., Taha, S.A. and Ibrahim, S.O. (2021). Electron Swarm Parameters and Dielectric Properties of the Superconducting Binary Mixtures of He-H_2. *Alinteri Journal of Agriculture Sciences, 36*(1): 420-432. doi: 10.47059/alinteri/V36I1/AJAS21063

Introduction

Hydrogen gas is a lightest diatomic gas, colorless, orderless, non-metallic, tasteless, high flammable, non-toxic but is asphyxiate by separation (up losing) oxygen in the air. Hydrogen gas used in several industrial application, i.e. maritime application, domestic energy, electricity generation and gas used in superconductor application (Berg, Palmer, Miller, Husband, & Dodds, 2015, Ganesh Babu Loganathan 2020; Ellappan Mohan, 2021).

* Corresponding author: muhamad.othman@su.edu.krd

Superconductor are materials with zero resistance was discovered by Kamerlingh in 1911, due to their critical temperature classified into two groups, first below 30K called low temperature superconductor (LTS), second above 30K are called high temperature superconductor (HTS). High temperature superconductor (HTS) technology used for power application useful in aerospace and naval applications; C. Kannan, and C.K. Kishore 2014.; S Priyadharsini 2014; Maheswari, V., Nandagopal 2016).

Gaseous helium (GHe) indicated cryogen for (HTS) power applications operate at temperature 77K to produce the higher critical current density studied by (Larbalestier, Gurevich, Feldmann, & Polyanskii, 2011). However, gaseous helium GHe choose as cooling media for certain high temperature superconducting HTS power applications, in which reduced asphyxiation hazard and wider operation temperature range (S Pamidi, Kim, & Graber, 2015, Nandagopal, Dr.V., Maheswari 2016). It is preferable to use (GHe) as a cryogen because of it's lower dielectric strength compared to that of liquid nitrogen (LN2), which limits the applicability of (GHe) to low voltage power devices (Rodrigo, Kwag, Graber, Trociewitz, & Pamidi, 2013; Shin, Hwang, Seong, Lee, & Lee, 2012). At cryogenic temperatures the dielectric strength of pure (GHe) lower than that of hydrogen gas, (L Graber et al., 2015, Dr.Mohammad, M. Othman. 2021) show a small mole fraction of H_2 in He-H_2 mixture increase ac breakdown voltage compared to pure GHe.

In Cryogenic He-H_2 mixtures the electron energy distribution function (EEDF) is most important parameters to calculate dielectric strength of gases and electron swarm parameters, i.e. electron mobility (μ_e), diffusion coefficient (D), mean electron energy (ε), characteristic energy (D/μ_e), drift velocity (v_d), ionization (α) and attachment (η) coefficient as well as the critical reduced electric field strength $(E/N)_{crt}$ at which the density-reduced ionization coefficient (α/N) and reduced attachment coefficient (η/N) are in balance ($\alpha/N= \eta/N$). All these parameters are calculated by the electric field strength E/N, using two-term approximation solution of Boltzmann equation analysis, where E is the applied electric field and N gas number density, E/N expressed in unit of Townsend (Td), where ($1Td=10^{-17}$ $V.cm^2$).

A number of workers have studied dielectric field strength of pure gases and mixtures under an applied dc electric field. For example, (Pinheiro & Loureiro, 2002, Loganathan, Ganesh Babu,2020, B.K. Patle, 2019, Dr. Othman, M.M., Ishwarya, K.R., 2021, Sai Krishnan G., 2019) studied the effective ionization coefficient (α-η/N) of hexafluoride and its mixtures with helium and xenon respectively. (Zhao, Li, Jia, & Murphy, 2014) investigated the critical reduced electric field strength for CO_2 and its mixtures with 50% O_2 and 50% H_2 from Boltzmann equation analysis at various gas temperature and atmospheric pressure, (Zhao & Lin, 2016) studied the breakdown properties of N_2-O_2 mixtures by taking into account the electron detachments from negative ions. (Li, Zhao, & Jia, 2012; Wang, Tu, Mei, & Rong, 2013; Zhong et al., 2014: R. Sujith Kumar, 2020; Dr.A. Senthil Kumar,2020; Sivam, S.P.S.S 2019) estimated the dielectric breakdown properties of SF_6 – N_2, SF_6 – He and SF_6-CO_2 mixtures at high temperature and pressure respectively, (Tezcan, Dincer, Bektas, & Hiziroglu, 2013) use the two-term solution of Boltzmann approximation solution to study the electron swarm parameters and dielectric strength in binary CF_4-CF_4 mixtures by variation the mole fraction of CF_4 in mixtures. (Deng, Li, & Xiao, 2015) conducted the Boltzmann equation analysis to analysis the insulation characteristic in binary gas mixtures of C_3F_8 with N_2 and CO_2. This studies were used non-cryogenic temperature to calculate transport parameters and density reduced critical electric field $(E/N)_{crt}$ and electric field E_{crt} by using two-term solution of Boltzmann solution analysis.

Although a lot of workers have used density reduced critical electric field $(E/N)_{crt}$ as a metric to calculate the dielectric strength of gas mixtures at cryogenic temperature (10-100K) and pressure used in HTS over the range 1.0 and 2.0 MPa. Hence, it is necessary to select the allowed mole fraction of gas mixtures to examine greater $(E/N)_{crt}$ over the cryogenic temperature range. The best choice gases for cryogenic applications are H_2, He, N_2, O_2, and F_2, the Paschen's curves in their pure form are widely available (Lieberman & Lichtenberg, 2005; Raizer, 1991). Most of the leaflet on dielectric strength is related to He and its potential replacements. Experimental and theoretical studies of swarm parameters and electric field strength at cryogenic temperature (HTS) have previously been published, for example, (Fitzpatrick, Kephartl, & Golda, 2007, Dr.Idris Hadi Salih, 2020) study the characterization of GHe for naval application of HTS, (L Graber et al., 2015, Ganesh Babu Loganathan 2020) measured the dielectric properties of two binary cryogenic gas mixture of He-H_2 and He-Ne, containing 4mol% hydrogen and 4 mol% Ne, respectively at temperature of 77 K over the gas pressure 0.5-2 MPa, (Park et al., 2016) studied the breakdown voltage and its application for binary He-H_2 cryogenic gas mixtures, (Peter Cheetham et al., 2016) investigated the dielectric strength binary He-H_2 cryogenic mixture both in ac and dc by increasing small mole fraction of hydrogen gas, (P Cheetham, Park, Kim, Graber, & Pamidi, 2017) studied the dielectric properties of He-H_2 cryogenic gas mixtures for superconducting power application, (Park, Pamidi, & Graber, 2017; A. Devaraju, 2020; Qaysar S. Mahdi 2018) studied the dielectric properties of He-H_2 cryogenic gas mixtures using Langmuir probe. Prototypes of gaseous helium at low temperature <77 K for superconducting power application explained by (Lukas Graber, Kim, Pamidi, Rodrigo, & Knoll, 2014; Sastry Pamidi, Kim, Kim, Crook, & Dale, 2012). To reduced risk of asphyxiation the US Navy has a priority in employing gaseous helium GHe instead of liquid nitrogen LN2 (Kephart et al., 2010). The influence of temperature on the dielectric strength of gaseous cryogenic media has been measured experimental over a wide range of temperature by (Park, Wei, et al., 2018), while the effect of magnetic electric field on the dielectric strength of gaseous helium as cooling media for superconducting applications was investigated experimentally by (Park, Cheetham, et al., 2018). The dielectric properties of binary He-H_2 and ternary He-H_2-N_2 gas cryogenic mixtures for superconducting power application in the temperature range 77-5000 K at 1.0-2.o MPa are obtained based on the Gibbs free energy minimization method by (Park, Pamidi, & Graber, 2018, Mohammed Abdulghani 2020).

Recently (Park et al., 2019, Ganesh Babu Loganathan 2019, Suganthi K, Idris Hadi Salih,2020) used Paschen's model for appreciation dielectric strength in pure gases as well as binary He-H_2 and ternary He-H_2-N_2 cryogenic gas mixtures.

The dielectric strength properties of pure gases and its mixtures have not been studied theoretically by using Boltzmann equation analysis. In this research, the electron swarm parameters of H_2 and He-H_2 mixtures were investigated using two term solution approximation of Boltzmann equation analysis at critical temperature (77 K) over the range $1 \leq E/N \leq 100$ Td, where ($1Td=10^{-17}$ $V.cm^2$). The density reduced ionization and attachment coefficient were calculated from the electron energy distribution function (EEDF). Finally, the density reduced critical electric field strength $(E/N)_{crt}$, when α/N equal to η/N, where N is the total number density.

Boltzmann Equation Analysis

The electron energy distribution function is important physical parameters used to calculate electron swarm parameters and reaction rate for electron collision reactions, can be calculated using two-term approximation solution of Boltzmann equation. The relationship between the electron swarm parameters and collision cross sections of electron with the neutral particles (elastic and inelastic) through the electron energy distribution function in below charts.

Consider an electron gas drifting in uniform dc applied electric field E, in V/cm with a velocity distribution f(v), the general form of the Boltzmann equation describes the evolution of the distribution function in six-dimensional space is (Hagelaar & Pitchford, 2005; Morgan & Penetrante, 1990; Xiao, 2016),

$$\frac{\partial f(v)}{\partial t} + v\nabla_r f(v) - \frac{eE}{m}.\nabla_v f(v) = \left(\frac{\partial f}{\partial t}\right)_{oll} \quad (1)$$

$$\left(\frac{\partial f}{\partial t}\right)_{coll} = \left(\frac{\partial f}{\partial t}\right)_{el} + \left(\frac{\partial f}{\partial t}\right)_{in} \quad (2)$$

Where, ∇_r is the space gradient operator in three dimensions ∇_v is velocity gradient operator in three dimensions, v is velocity and. $\left(\frac{\partial f}{\partial t}\right)_{coll}$ is collision operator due to elastic and inelastic collisions of electron with the neutral particles such as excitation, ionization and attachment. When space gradient are negligible $f(r,\bar{v},t) = f(\bar{v},t)$, $\nabla_r f = 0$ and equation for one kind of particle can be written as, [4],

$$\frac{\partial f(v)}{\partial t} - \frac{eE}{m}.\nabla_v f(v) = \left(\frac{\partial f}{\partial t}\right)_{coll} \quad (3)$$

To solve equation (3), the distribution function *f(v)* expand in term of spherical Legendre functions,

$$f(\bar{v}) = \sum_{\lambda=0}^{\infty} f_\lambda(v) P_\lambda(\cos\theta) \quad (4)$$

only the first two term approximation of distribution function *f(v)* considered, when the mean random velocity greater than drift velocity (Jiang & Economou, 1993),

$$f(\bar{v}) = f_o(v) + \frac{\bar{v}}{v} f_1(v) \quad (5)$$

Where, $f_o(v) << f_1(v)$, $f_o(v)$ and $f_1(v)$ are isotropic and anisotropic part respectively, obtained by substituting equation (5) into equation (3), leads to form two coupled equations (Jiang & Economou, 1993),

$$\frac{-\partial f_1}{\partial t} + \frac{eE}{m}\frac{\partial f_o}{\partial v} = \frac{f_1}{\tau} \quad (6)$$

$$\frac{\partial f_o}{\partial t} - \frac{1}{mv^2}\frac{\partial}{\partial v}\left(\frac{ev^2}{3}E.f_1 + \frac{m^2}{M}NQ_m v^4 f_o + \frac{mK_BT}{M}NQ_m v^3 \frac{\partial f_o}{\partial v}\right) = \left(\frac{\partial f_o}{\partial t}\right)_{in} \quad (7)$$

in equation (7), The right term $\left(\frac{\partial f_o}{\partial t}\right)_{in}$ indicates to inelastic collision only, τ is relaxation time in picoseconds, assume that all quantities in equation (6) are independent of time, the solution is,

$$f_1 = \frac{eE\left(\frac{\partial f_o}{\partial v}\right)}{mNvQ_m} + \exp\left(-\frac{t}{\tau}\right) \quad (8)$$

$$\tau = \left(NvQ_m\right)^{-1} \quad (9)$$

during this time scale the value E or N do not change, then f_1 is given,

$$f_1 = \frac{eE\left(\frac{\partial f_o}{\partial v}\right)}{mNvQ_m} \quad (10)$$

Making a change in the independent variable $u=mv^2/2e$, the steady state electron energy distribution function *f(u)* obtained by solution of the Boltzmann equation may be written in the form (Frost & Phelps, 1962; Holstein, 1946; Margenau, 1946).

$$\frac{E^2}{3}\frac{d}{du}\left(\frac{u}{NQ_m(u)}\frac{df_0(u)}{du}\right)+\frac{2m}{M}\frac{d}{du}\left(u^2NQ_m(u)f_0(u)\right)$$
$$+\frac{2mK_BT_g}{Me}\left(u^2NQ_m(u)\frac{df_0(u)}{du}\right) \quad (11)$$
$$+\sum_J\left[(u+u_J)f_o(u+u_J)N_oQ_J(u+u_J)-uf_o(u)N_oQ_J(u)\right]$$
$$+\sum_J\left[(u-u_J)f_o(u-u_j)N_JQ_{-J}(u-u_J)-uf_o(u)NQ_{-J}(u)\right]=0$$

Here, e, m, M, K_B, and u are the electron charge, electron mass, molecular mass, Boltzmann constant and electron energy respectively, N is the number density of molecules per cm^3. $Q_m(u)$ is the momentum transfer cross-sections related to the total cross section $Q_m(u)= Q_T(u)(1\text{-}\cos\theta)$, where θ is scattering angle (Lucas, Price, & Moruzzi, 1973). $Q_J(u)$, and u_J are, excitation (rotational, vibrational, electronic) cross-section and energy loss due to collisional excitation respectively. The last two term is the influence of superelastic collision it occurs at low electric field, $Q_{-J}(u)$ is superelastic cross-section, u_J energy gain due to superelastic collision.

The superelastic cross-section Q_{-J} can be written as (Mitchell & Zemansky, 1934),

$$Q_{-J}=\frac{u+u_J}{u}Q_J(u+u_J) \quad (12)$$

The electron energy distribution function (EEDF) was obtained by using equation (11) known as the Holstein form (Holstein, 1946) which plays an important physical parameter for calculating the electron swarm parameters and reaction rates. At low electron energy and thermal equilibrium, the elastic collision are dominated, otherwise the effect of inelastic collision (excitation and ionization) required higher electron energy to occur, play the main role in the dropping of EEDF or shifting to left or right coincide to decreasing or increasing of mean electron energy and kind of gas mixtures.

In the case of thermal equilibrium the EEDF was chosen as Maxwellian function (Nighan, 1970), with temperature T_e is given by,

$$f(u)=\frac{2}{\sqrt{\pi}}.\sqrt{\frac{1}{(K_BT_e)^3}}.\sqrt{u}.\exp\left(\frac{u}{K_BT_e}\right) \quad (13)$$

With mean electron energy,

$$\bar{u}=\frac{3}{2}K_BT_e \quad (14)$$

where K_B is Boltzmann constant, equal to one when electron temperature expressed in unit of energy (in eV). The EEDF normalized by,

$$\int_0^\infty \sqrt{u}\,f_o(u)du=1 \quad (15)$$

The electron swarm parameters are expressed in terms of electron energy distribution function EEDF ($f_o(u)$ in $eV^{-3/2}$) and total effective momentum transfer cross-section as follows (M. Viswanathan, (2020); Mohammad M Othman, Taha, & Sailh, 2019),

The mean electron energy (eV),

$$\bar{u}=\int_0^\infty u^{\frac{3}{2}}f_o(u)du \quad (16)$$

The electron mobility (cm^2/V. s),

$$\mu_e=-\frac{1}{3N}\left(\frac{2e}{m}\right)^{1/2}\int_0^\infty\frac{u}{Q_T(u)}\frac{df_o(u)}{du}du \quad (17)$$

The electrons drift velocity (cm/s),

$$v_d=\mu_eE \quad (18)$$

The diffusion coefficient (cm^2/s),

$$D_T=\frac{1}{3N}\left(\frac{2e}{m}\right)^{1/2}\int_0^\infty\frac{uf_o(u)}{Q_T(u)}du \quad (19)$$

Here, $Q_T(u)$ is total effective momentum transfer cross-section, given by,

$$Q_T(u)=Q_{ela.}(u)+\sum Q_{inel.}(u) \quad (20)$$

where, $Q_{ela.}(u)$ elastic (momentum transfer) cross sections, the term $\sum Q_{inel.}(u)$ includes all the excitation cross-sections of discrete (rotational, vibrational, electronic) states.

The reduced density ionization coefficient (cm^2) is given by (Hagelaar & Pitchford, 2005; Laska, Mašek, Krasa, & Peřina, 1984; Mohammad M Othman, Taha, & Salih, 2019),

$$\frac{\alpha}{N}=\frac{1}{v_d}\left(\frac{2e}{m}\right)^{1/2}\int_i^\infty Q_i(u)uf_o(u)du \quad (21)$$

where $Q_j(u)$ is the ionization cross-section.
The reduced density attachment coefficient (cm^2) is given by,

$$\frac{\eta}{N}=\frac{1}{v_d}\left(\frac{2e}{m}\right)^{1/2}\int_a^\infty Q_a(u)uf_o(u)du \quad (22)$$

where $Q_a(u)$ is the attachment cross-section.

The reduced critical electric field strength $(E/N)_{crt.}$ is obtained when the creation and loss electrons reach a balance,

$$\frac{\alpha}{N}=\frac{\eta}{N} \quad (23)$$

In this case the effective ionization coefficient $\alpha_{eff.}=(\alpha-\eta)/N$ equal to zero (Itoh, Shimozuma, & Tagashira, 1980).

For the present work the EEDF and drift velocity dependent on elastic (momentum transfer) cross section

($Q_{ela}(u)>>Q_{inela}(u)$) and its variation with energy, the inelastic collision prevents electrons from reaching high energies.

The values of electron energy distribution function as a function of electron energy *f(u)* are obtained from Boltzmann's equation using all the electron collisional cross-sections.

Cross Section

The data of electron collision cross-sections which is the interaction between electrons and neutral gases is the most fundamental factor, used as input data to calculate electron swarm parameters in He-H_2 mixtures using two-term approximation solution of Boltzmann equation. The elastic and inelastic cross-sections used in the present analysis are explained below. The set cross-sections for H_2 molecule includes one momentum transfer cross- section determined by (Gibson, 1970)), three vibrational excitation cross-section (v_1, v_2, v_3) with threshold energy 0.027, 1.03 and 1.864 eV respectively, determined by (Ehrhardt, Langhans, Linder, & Taylor, 1968), two electronic excitation cross-section with threshold energy of 8.85 eV and 12.0 eV determined by (Engelhardt & Phelps, 1963), one dissociative attachment cross section with threshold energy 3.56 eV taken from (Yoon et al., 2008), and one ionization cross section with threshold energy 15.427 eV determined by (Rapp & Englander-Golden, 1965).

The set of collisional cross-sections for He atom includes one momentum transfer cross-section taken from (Crompton, Elford, & Robertson, 1970), three electronic excitation cross-section (${}_{2}^{1}P$, ${}_{2}^{3}P$) with threshold energy 21.203 eV and 20.949 eV respectively determined by (Jobe & John, 1967) and (${}_{3}^{1}P$) with threshold energy 23.071 eV determined by (Van Eck & De Jongh, 1970), and one ionization cross-section with threshold energy 24.586 eV taken from (Rapp & Englander-Golden, 1965). In the present work, we used the two- term solution of Boltzmann equation for the energy given by (Rockwood & Greene, 1980), this method was used in our previous works (Mohammad Mustafa Othman, Taha, & Mohammad, 2017). Therefore, the calculated electron swarm parameters by using H_2 and He cross-section, which include electron drift velocity, diffusion coefficient, electron mobility, mean electron energy, ionization coefficient, attachment coefficient and reduced critical electric field strength in He-H_2 gas mixture.

Results and Discussion

Hydrogen is an active and main attaching gas in the He-H_2 gas mixture, it differs from the helium gas that has vibrational levels and dissociation attachment. To solve the electron energy distribution function (EEDF) based on the two-term solution of Boltzmann equation, the data of electron collision cross-sections of He and H_2 are explained in previous section, used as main input data to calculated electron swarm parameters.

This calculation focused on the density reduced ionization and attachment coefficient although the density reduced critical electric field strength $(E/N)_{crt}$ in He-H_2 mixtures in the range from 1 to 100 Td at critical temperature 77 K and pressure 2 MPa. The mixing ratio of the H_2 in mixtures select from 20% H_2 to 1% H_2.

The electron energy distribution function EEDF as function of electron energy, are obtained by using two-term approximation solution of Boltzmann equation method (Eq. 11), at different values of electric field strength E/N (E: electric field, N: gas number density). Electric field strength E/N, expressed in unit of Townsend (Td) is equal to 10^{-17} V.cm^2.

The calculated EEDF for a dc field in H_2 and He at different values of E/N at temperature 77K and pressure 2MPa are shown in figures 1 and 2 respectively. It is found that at lowest electric field strength E/N, the electron energies are thermal and the electron energy distribution function EEDF is Maxwellian (Eq. 13) with mean electron energy $\bar{u} = 1.5 K_B T_e$, the Maxwellian distribution function normalized by Eq. 15, where T_e is in unit of eV, and decrease sharply at after several (eV). When E/N<17 Td for pure H_2 and E/N≤2 Td for pure He, the Maxwellian function's will appear as straight lines, because the elastic and inelastic cross-section is constant at low electric field, in this region the degree of ionization is very small. However, for higher E/N values the EEDF in H_2 and He is clearly non-Maxwellian, and has a shoulder at about 3 eV when E/N≥10 Td, due to the large electronic excitation and vibrational cross-section, in the case of H_2 the vibrational cross-section is equal to 5.1x10^{-16} cm^2 at 3 eV. As shown in figures 1and 2, the tail of the distribution function shifts to higher energy due to inelastic collision which reflect the dominant electron-molecule energy exchange processes in this region more ionization or excitation collision occurs, then the mean electron energy increases with increasing E/N, as shown in figure 3. Whenever for different concentration of He and H_2 gas mixtures along with the H_2 and He are appearing, the relation of EEDF as function of electron energy for a fixed value of E/N=10 Td at temperature 77K and pressure 2 MPa, are shown in figure 4. The pure H_2 has higher EEDF at lower electron energy compared with He. The EEDF have been effect by adding small mole fractions of H_2 in the He-H_2 gas mixture. For electron energy ≤3 eV, the EEDF increase with increasing H_2 mole fraction in the mixture. However, at electron energy > 3 eV the EEDF decreases and the tail shifted to the left, this is because the threshold energy at the vibration level (v_1) is 0.027 eV in the case of H_2 gas, for this reason the inelastic collision of electrons with H_2 molecules occurs at low E/N values, there are only little number of electrons that have energies greater than the ionization potential. As the ratios of H_2 in the mixture increases, the degree of ionization and the number of particles with energies higher than excitation energy decreases tends to increase the attachment process.

To emphasize the validity of two-term solution of Boltzmann equation analysis, the electron drift velocity, and reduced density ionization coefficient values of the present study were compared with previous experimental and theoretical literatures. The values of drift velocity of H_2 at temperature 77 K as a function of E/N are shown in figure 5, the present results are compared with the experimental values of (Roznerski & Leja, 1984) and theoretical values of

(Engelhardt & Phelps, 1963; Raju, 2018; Thi Lan & Jeon, 2012). The present results agree will over the common E/N range. The present values of drift velocity for He are shown in figure 6, along with the previous experimental values of (Kucukarpaci, Saelee, & Lucas, 1981) and theoretical values of (Raju, 2018; Tuan, 2016) are in good agreement for comparison. It is evident that the experimental data of (Pack, Voshall, Phelps, & Kline, 1992) fall below present results, the difference increases up to about 9% over the range of E/N>6 Td.

The density reduced ionization coefficient α/N were calculated at temperature 77K and pressure 2MPa, by using two-term solution of Boltzmann equation. In the case of H_2 results were taken over the range 45≤E/N≤100 Td. Figure 7 shows α/N as function of E/N, together in comparison with experimental values of (Crompton, Dutton, & Haydon, 1955; Rose, 1956; Shallal & Harrison, 1971) and theoretical values of (Engelhardt & Phelps, 1963; Lieberman & Lichtenberg, 2005; Raju, 2018), good agreement has been observed. Figure 8 shows α/N in He over the range 10≤E/N≤100 Td, measure values of (Chanin & Rork, 1964; Davies, Jones, & Morgan, 1962; Dutton, 1975) and theoretical values of (Lieberman & Lichtenberg, 2005; Raju, 2018) are also plotted for comparison. The agreements are good, while at high E/N≥145 Td the experimental values of (Lakshminarasimha, Lucas, & Snelson, 1975) are lower than present results. The coherent results obtained confirmed that two-term solution of Boltzmann equation analysis of the present study is valid.

Flammability is a risk factor for hydrogen gas under atmospheric pressure and ambient temperature. To study dielectric strength of He-H_2 cryogenic gas mixture, before adding H_2 into He one should consider the flammable conditions fail to propagate a flam in the mixtures. The values of the flammability limits of He-H_2 cryogenic gas mixtures are presented in figure 9, and listed in table 1 (Terpstra, 2012). For mixtures with small concentration of H_2 over the range 1% to 9% safe flammability limits were observed.

Figure 10 shows the mean electron energy as a function of H_2 content in He-H_2 mixtures for fixed value of E/N=10 Td, the mean energy is a summary of the electron energy distribution function under specified conditions. Variation of mean energy of binary He-H_2 cryogenic gas mixtures as function of E/N are presented in figure 11. The mean electron energy increases with increasing E/N, whereas, the tail of EEDF shifts to lower energy when the mole fraction of H_2 increase in the binary He-H_2 cryogenic gas mixtures, the mean electron energy of the mixtures has a trend of decreasing with increasing H_2 content. The results show a negative relation between the mean energy of the He-H_2 cryogenic gas mixtures and the mole fraction of H_2.

The dependence of reduced electron mobility $N\mu_e$ on reduced electric field E/N for different mole fraction of H_2 in cryogenic gas mixtures is represented in figure 12. At low E/N values the behavior of the electron mobility decreases with increasing H_2 concentration at specified E/N values. While, at interval E/N>10 Td the behavior of electron mobility reversed by increasing small mole fraction of H_2. As shown in figure 4, at specified E/N=10 Td, the increase of H_2 concentration alters the EEDF by shifting it to lower energies, results in decreasing mean electron energy, which effected the behavior of electron mobility, diffusion coefficient, ionization and attachment coefficient.

The diffusion coefficient ND_T as a function of E/N for pure H_2, He and binary He-H_2 gas mixture is presented in figure 13. The behavior of diffusion coefficient increase with increasing E/N, while the negative correlation of the diffusion coefficient with the mole fraction of hydrogen at fixed value of E/N in the binary He-H_2 cryogenic gas mixture as shown in figure. The diffusion coefficient of pure H_2 lower than He, this difference refers to collisional electron cross-sections. Inelastic cross-sections (excitation, ionization and attachment cross –sections) require higher electron energy compared to elastic cross-sections [$(2m/M) \leq 10^{-4}$, where m is electron mass and M is molecule/atom mass], which effect the kinetic of electrons and EEDF.

Reduced electric field strength E/N as well as structure of a gas mixture effect the EEDF. All gases which display with high dielectric field strength, the tail of EEDF shifted to the lower energy region. Figure 14 represented reduced density ionization coefficient α/N values of He-H_2 cryogenic gas mixture as a function of E/N, calculated values based on EEDF by using two-term approximation solution of Boltzmann equation analysis (Eq. 11), using all types of collision cross-sections. The negative correlation of reduced density ionization coefficient α/N appears with increasing H_2 ratio in the mixture, also the calculated α/N values of He and H_2 together are shown in the same figure. In comparison the α/N in H_2 is lower than the value of He, over the same entire range there are seven curves lie between He and H_2 with different ratio of H_2, i.e., 1%, 3%, 5%, 7%, 10%, 15%, and 20%. As shown in figure 14, increasing the ratio of H_2 in the mixture, leads to decreasing ionization coefficient of mixture. It is well known the growth of the inelastic collisions are depend on electron energy and the hydrogen ratio in the mixture, for example the threshold energy of ionization potential is 15.427 eV, occurs at high electron energy, tends to reduce the number of fast electrons, decreasing mean electron energy results the tail of EEDF shifted to the lower energy region, give rise lowering the Townsend ionization coefficient as the mole fraction of hydrogen gas increased in the binary He-H_2 cryogenic gas mixture.

The reduced density attachment coefficient η/N in He-H_2 mixture is shown as a function of E/N for different ratio H_2 in figure 15. The value of η/N increases to maximum value and start to decrease with increasing E/N. The behavior is observed with all values of H_2 mole fraction in binary He-H_2 cryogenic gas mixtures, the maximum value are variant between 15 Td to 40 Td, due to diffusion loss in the mixture, when He is used as the buffer gas has zero attachment cross-section, which means that electron cannot attach to helium atom to form negative ions. Then the energy gains and losses are dominated by helium momentum transfer cross-sections. On the other hand, a positive correlation of η/N shown in figure (direction of the arrow) by increasing the amount of hydrogen in binary mixture. However, the large collision ionization cross-section of helium and the small collision ionization cross-section of hydrogen, and different excitation collision cross-section of hydrogen are contributes to create reduced density attachment coefficient η/N by shifting the tail of electron energy distribution function EEDF to lower energy region, it is the condition that attachment collision happen at low electron energy. Further decreasing the value of α/N with the ratio of H_2 in the binary mixture, leads to increase the value of η/N.

Based on the values of density-reduced ionization coefficient α/N and density-reduced attachment coefficient η/N, the density-reduced effective ionization coefficient (α-η)/N can be predicate, is obtained, at which α/N and η/N are exactly balanced, (α-η)/N=0, this method used by (Itoh et al., 1980; Mohammad M Othman, Taha, & Salih, 2019; Qin et al., 2019). From the curves of (α-η)/N as function of E/N, the density-reduced critical electric field $(E/N)_{crt.}$ and critical breakdown electric field $E_{crt.}$ are defined as the E/N values at which (α-η)/N=0.

Figure 16 illustrated density-reduced effective ionization coefficient (α-η)/N as function of E/N in He-H_2 cryogenic gas mixtures at the ratio of 99/1, 97/3, 95/5, 93/7, 90/10, 85/15 and 80/20. With increasing H_2 mole fraction, the value of $(E/N)_{crt}$ is strongly increased. Based on the data illustrated in figure 16 we can calculate that the value of $(E/N)_{crt}$ increases from 7.5 Td to 20.4 Td, as the mole fraction increases from 1% to 80%. Thus, it is clear that the increases of H_2 mole fraction in mixture will significantly increase the probability of dielectric breakdown occurring in the binary He-H_2 cryogenic gas mixture at a fixed gas pressure 2MPa and temperature 77K, including the vibrational kinetics resulting higher critical breakdown electric field, so the net electron production by ionization process is low at high E/N, resulting high higher critical breakdown electric field.

The density-reduced critical electric field strength $(E/N)_{crt}$ for the He-H_2 cryogenic gas mixtures as function of H_2 content at pressure 2 MPa and temperature 77K are presented in figure 17 and listed in table 2. It can be shown that as H_2 content increases, so that the reduced critical electric field $(E/N)_{crt}$ increases. Note that the critical breakdown electric field $E_{crt.}$ for pure helium is not listed in table, because in helium η/N=0. In addition, the value of critical breakdown electric field $E_{crt.}$ for 94/5 He-H_2 mixture equal to 9.87 x 10^4 V/cm, were in good agreement within the range of experimental breakdown voltage values of (Peter Cheetham et al., 2016; L Graber et al., 2015; Park et al., 2016). While, the real value of breakdown voltage of a mixture include secondary electron emission coefficient γ, according to relation $\gamma \exp(\alpha d) = 1 + \gamma^{-1}$ known as the Townsend breakdown criterion (Küchler, 2017), this value is not taken into account by theoretical study using two-term approximation solution of Boltzmann equation analysis. Therefore, the present value of critical breakdown electric field E_{crt} is in good agreement with experimental values. $E_{crt.}$ shows the dielectric strength, obtained when $(E/N)_{crt.}$ multiply by number density N. Note that the number density N is calculated by using ideal gas law N= P/K_BT, where, P is the absolute pressure of a gas and T is absolute temperature, and K_B is Boltzmann constant =1.38 x 10^{-23} J/K.

In addition, the dielectric strength value of 95/5 He-H_2 at two different pressures as a function of temperature is shown in figure 18. The dielectric strength decreases by increasing temperature because the dissociation process increases with increasing temperature. Otherwise, the dielectric strength at pressure 2.0 MPa has higher value compare with pressure 1.01 x 10^5 KPa at the same temperatures.

Table 1. Flammability limits of He-H_2 mixtures in air at T= 20°C.

He in the fuel mixture % by vol.	Lean Limit	Rich Limit
0	3.9	74.1
20	4.8	75.3
40	6.6	76.3
50	8.0	77.6
60	10.0	77.5
80	21.9	78.5
90	53.0	79.0
91	61.1	79.0

Table 2. Critical electric field strength and electric field strength at temperature 77 K and pressure 2 MPa for different He-H_2 mixtures.

He-H_2 mixture (mol%)	N (cm^{-3}) 10^{21}	$(E/N)_{crt.}$ 10^{-17} Vcm^2	$E_{crt.}$ (V/cm) 10^5
99/1	1.882	7.5	1.411
97/3	1.882	8.8	1.656
95/5	1.882	10.5	1.976
93/7	1.882	11.6	2.183
90/10	1.882	13.7	2.578
85/15	1.882	15.9	2.992
80/20	1.882	20.4	3.839

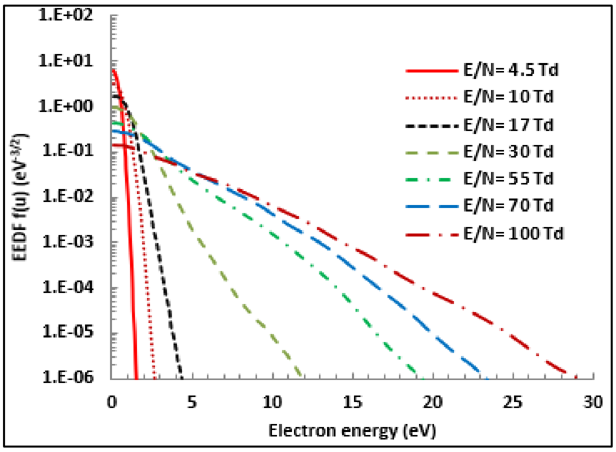

Figure 1. Electron energy distribution function as a function of electron energy for pure H_2 at T= 77k

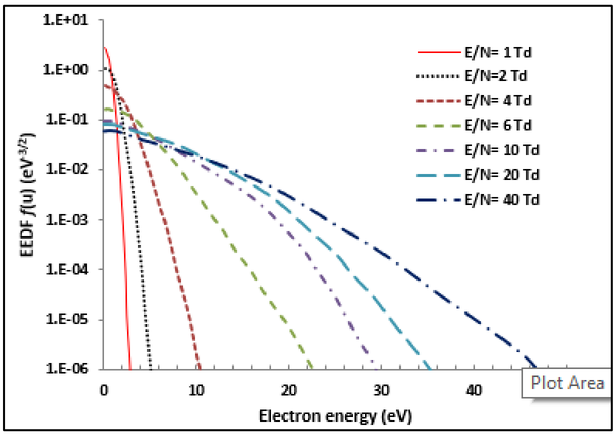

Figure 2. Electron energy distribution function as a function of electron energy for pure He at T= 77K

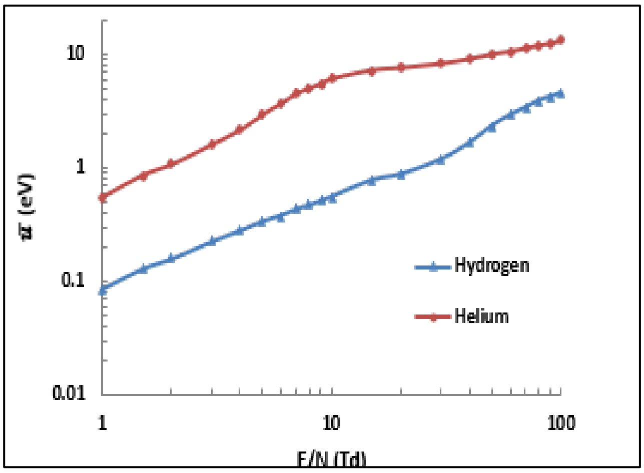

Figure 3. Mean electron energy as a function of electron energy

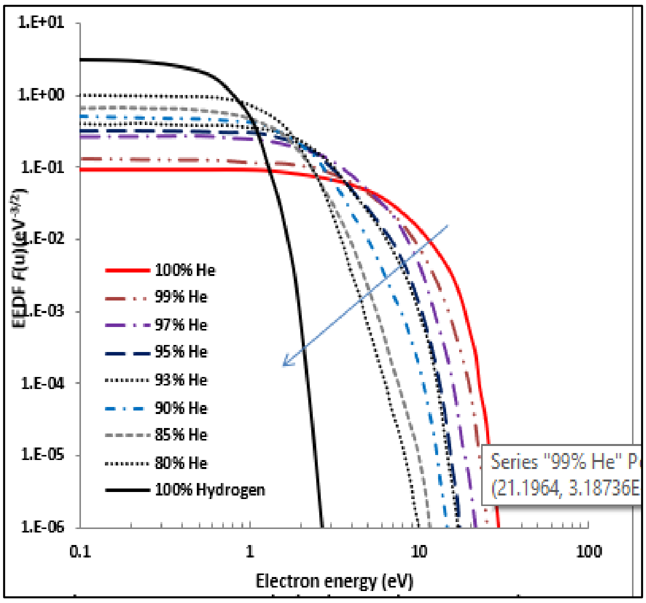

Figure 4. Electron energy distribution function for He- H_2 mixture at E/N-10 Td

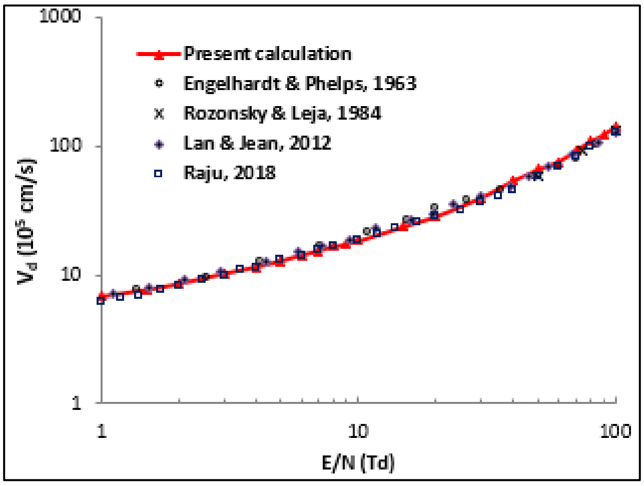

Figure 5. Electron drift velocity in pure hydrogen

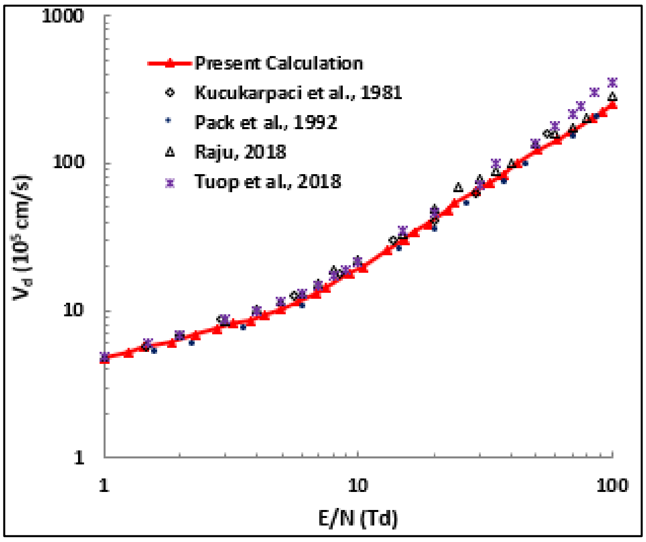

Figure 6. Electron dritt velocity in pure helium

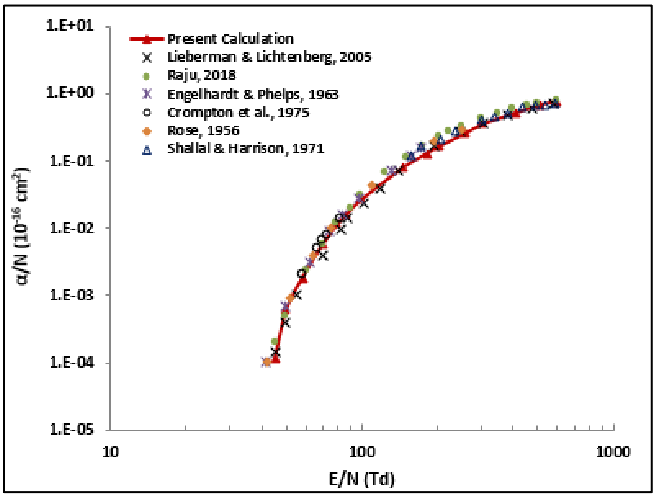

Figure 7. Density-reduced ionization coefficient in pure hydrogen

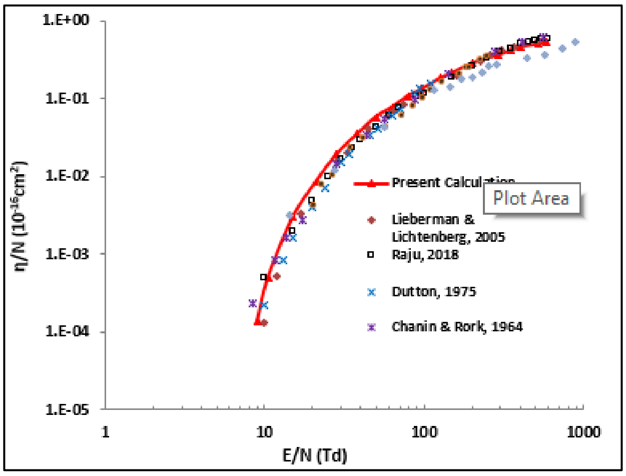

Figure 8. Density-reduced ionization coefficient in pure helium

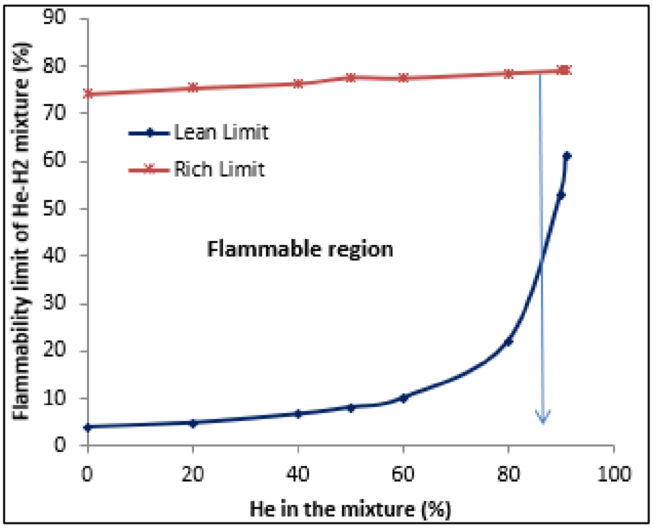

Figure 9. Flammability limits of He-H_2 mixtures in air as a function values from reference (Terpstra, 2012)

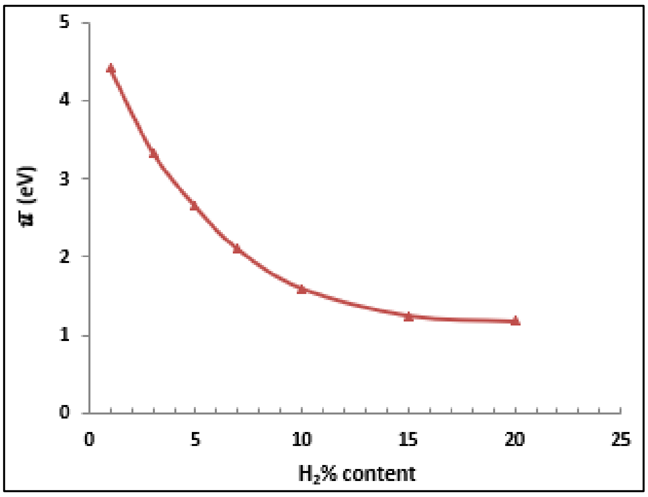

Figure 10. mean electron energy in He-H_2 mixtures as a function of H_2% content at E/N-10 Td.

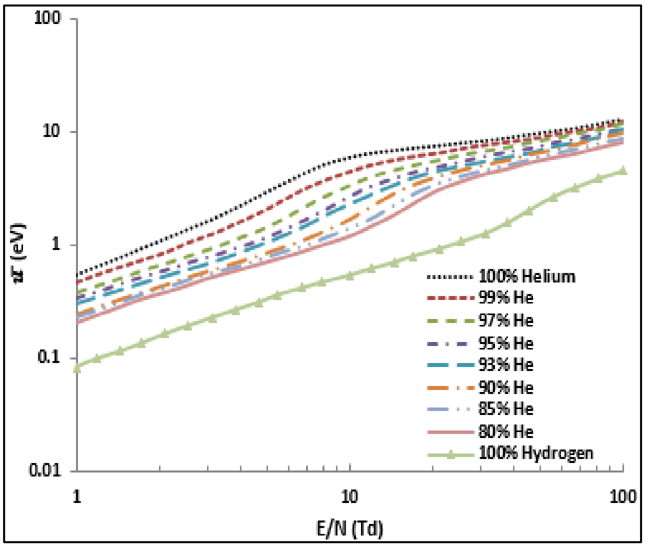

Figure 11. Mean electron energy in He-H_2 mixtures

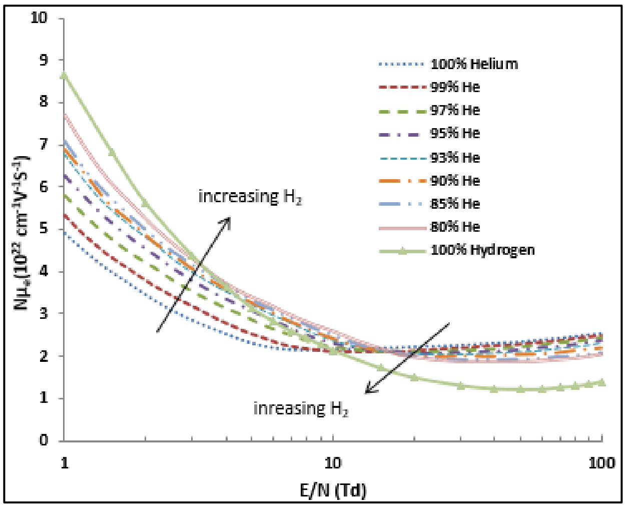

Figure 12. Density – normalized electron mobility in He-H_2 mixtures

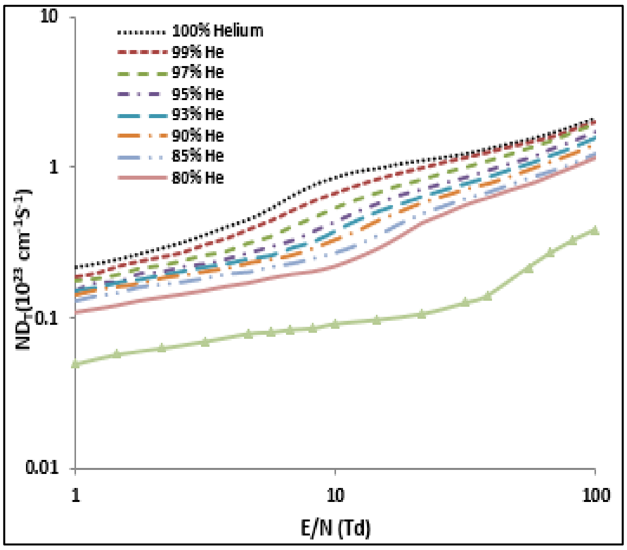

Figure 13. Density – normalized transverse diffusion coefficient in He-H_2 mixture

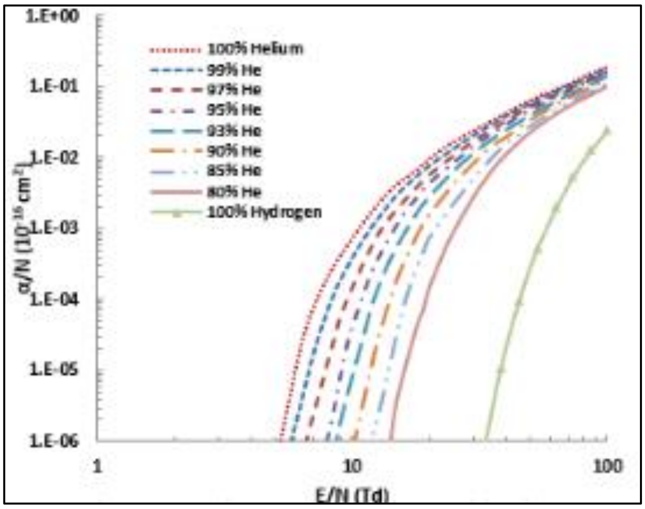

Figure 14. Density – reduced ionization coefficient in He-H_2 mixture

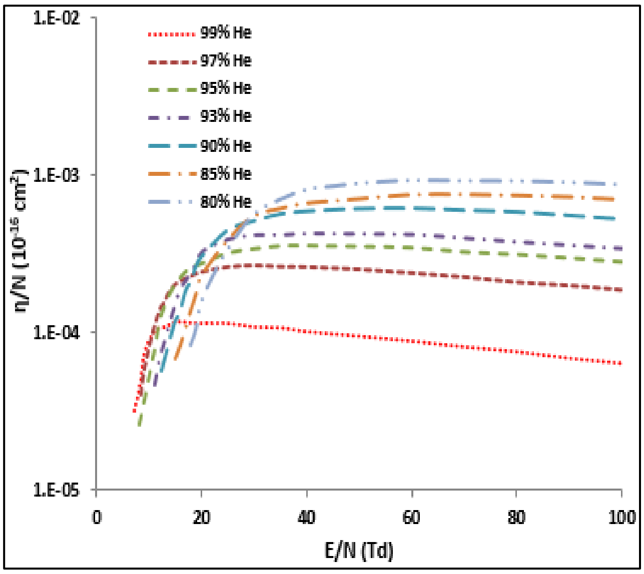

Figure 15. Density-reduced I attachment coefficient in He-H_2 mixtures

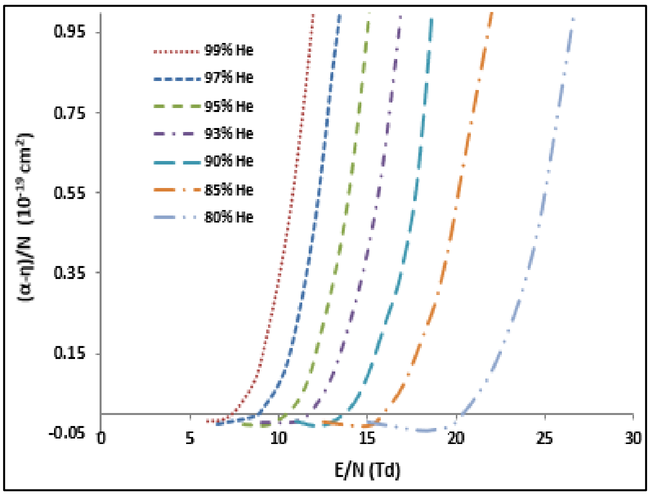

Figure 16. Density-reduced effective ionization coefficient in He-H_2 Mixtures

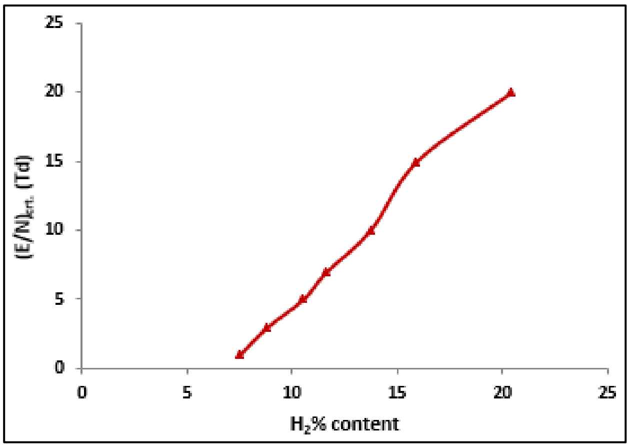

Figure 17. Density-reduced critical electrical field as a function of H_2% content in He-H_2 mixture at T=77 and P=2 Mpa.

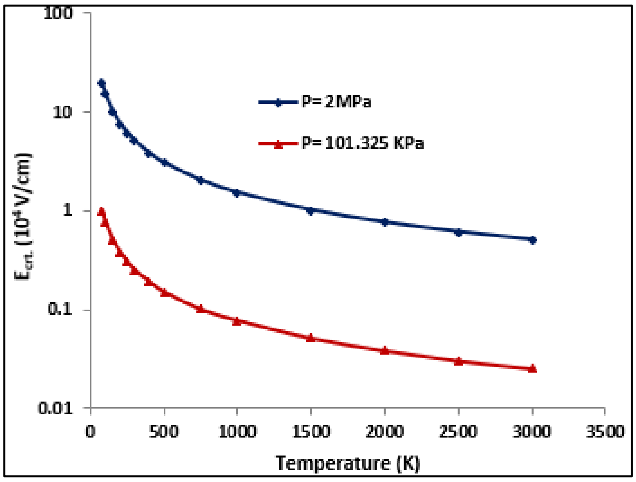

Figure 18. Critical electrical field as a function of pressure and temperatures for 95% He-5% H_2.

Conclusion

In this paper the EEDF and electron swarm parameters (electron drift velocity, mean electron energy, electron mobility diffusion coefficient, ionization and attachment coefficient, density-reduced effective ionization coefficient, reduced critical electric field and critical electric field) in binary of H_2 gas with buffer He gas was calculated and analyzed by a two-term approximation of Boltzmann equation over the range E/N varying 1 to 100 Td at temperature 77 K and pressure 2 MPa. The change in the number of electron density (i.e. electron ionization and attachment) have been taken into account to calculate EEDF, also the set of different cross sections play an important parameter for calculation the electron swarm parameters. The validity of the two-term approximation of Boltzmann equation in pure He and H_2 is confirmed over the entire range of E/N values, it is necessary to increase the momentum transfer cross-section slightly in order to obtain a good agreement between the present and previous theoretical and experimental results. In pure He and H_2 the calculated electron swarm parameters (v_d, α/N and η/N) in pure He and H_2 are in good agreement in comparison with available experimental and theoretical results. In the case of binary He-H_2 cryogenic gas mixture, the tail of EEDF shifted to lower energy region as the ratio of H_2 content in mixture increase, α/N, (α-η)/N decreases, while, η/N, $(E/N)_{crt.}$ and $E_{crt.}$ Increases. The present result of critical field strength $E_{crt.}$= 9.8 x 10^4 V/cm is within the range of previous experimental value. It is found that higher $E_{crt.}$ is obtained at higher pressure 2.0 MPa and lower temperature 77K. Furthermore, the mean electron energies at constant E/N value, decreases with increasing H_2 in the mixture.

Therefore, the present study is useful for several industrial applications, i.e. dielectric design of cryogenic switcher, arc discharge and development high-temperature superconductivity applications.

References

Berg, F., Palmer, J., Miller, P., Husband, M., & Dodds, G. (2015). HTS electrical system for a distributed propulsion aircraft. *IEEE Transactions on Applied Superconductivity, 25*(3), 1-5.

Chanin, L.M., & Rork, G. (1964). Experimental determinations of the first Townsend ionization coefficient in helium. *Physical Review, 133*(4A), 1005.

Cheetham, P., Kim, W., Kim, C.H., Graber, L., Rodrigo, H., & Pamidi, S. (2016). Enhancement of dielectric strength of cryogenic gaseous helium by addition of small mol% hydrogen. *IEEE Transactions on Applied Superconductivity, 27*(4), 1-5.

Cheetham, P., Park, C., Kim, C., Graber, L., & Pamidi, S. (2017). Dielectric properties of cryogenic gas mixtures for superconducting power applications. Paper presented at the *IOP Conference Series: Materials Science and Engineering.*

Crompton, R., Dutton, J., & Haydon, S. (1955). Growth of Pre-Breakdown Ionization Currents in Hydrogen. *Nature, 176*(4492), 1079-1079.

Crompton, R., Elford, M., & Robertson, A. (1970). The momentum transfer cross section for electrons in helium derived from drift velocities at 77 K. *Australian Journal of Physics, 23*(5), 667-682.

Davies, D.K., Jones, F.L., & Morgan, C. (1962). Primary ionization coefficient of helium. *Proceedings of the Physical Society, 80*(4), 898.

Deng, Y., Li, B., & Xiao, D. (2015). Analysis of the insulation characteristics of C 3 F 8 gas mixtures with N 2 and CO 2 using Boltzmann equation method. *IEEE Transactions on Dielectrics and Electrical Insulation, 22*(6), 3253-3259.

Dutton, J. (1975). A survey of electron swarm data. *Journal of Physical and Chemical Reference Data, 4*(3), 577-856.

Ehrhardt, H., Langhans, L., Linder, F., & Taylor, H. (1968). Resonance scattering of slow electrons from H2 and CO angular distributions. *Physical Review, 173*(1), 222.

Engelhardt, A., & Phelps, A. (1963). Elastic and inelastic collision cross sections in hydrogen and deuterium from transport coefficients. *Physical Review, 131*(5), 2115.

Fitzpatrick, B.K., Kephartl, J.T., & Golda, E.M. (2007). Characterization of gaseous helium flow cryogen in a flexible cryostat for naval applications of high temperature superconductors. *IEEE transactions on applied superconductivity, 17*(2), 1752-1755.

Frost, L., & Phelps, A. (1962). Rotational excitation and momentum transfer cross sections for electrons in H2 and N2 from transport coefficients. *Physical Review, 127*(5), 1621.

Gibson, D. (1970). The cross sections for rotational excitation of H2 and D2 by low energy electrons. *Australian Journal of Physics, 23*(5), 683-696.

Graber, L., Kim, C.H., Pamidi, S.V., Rodrigo, H., & Knoll, D. (2014). Dielectric design validation of a helium gas cooled superconducting DC power cable. Paper presented at the 2014 *IEEE Electrical Insulation Conference (EIC).*

Graber, L., Kim, W., Cheetham, P., Kim, C., Rodrigo, H., & Pamidi, S. (2015). Dielectric properties of cryogenic gas mixtures containing helium, neon, and hydrogen. Paper presented at the *IOP Conference Series: Materials Science and Engineering.*

Hagelaar, G., & Pitchford, L. (2005). Solving the Boltzmann equation to obtain electron transport coefficients and rate coefficients for fluid models. *Plasma Sources Science and Technology, 14*(4), 722.

Ganesh Babu Loganathan, Praveen M., Jamuna Rani D. Intelligent classification technique for breast cancer classification using digital image processing approach. *IEEE Xplore Digital Library* 2019, 1-6.

M. Viswanathan, Ganesh Babu Loganathan, and S. Srinivasan. IKP based biometric authentication using artificial neural network. *AIP Conference Proceedings* (2020), *2271*(1), 030030.

Mohammed Abdulghani Taha and Ganesh Babu Loganathan, Hybrid algorithms for spectral noise removal in hyper spectral images. *AIP Conference Proceedings* (2020), *2271*(1), 030013.

Dr.Idris Hadi Salih, Ganesh Babu Loganathan, Induction motor fault monitoring and fault classification using deep learning probablistic neural network. *Solid State Technology*(2020), *63*(6), 2196-2213.

Ganesh Babu Loganathan Design and analysis of high gain Re Boost-Luo converter for high power DC application. *Materials Today: Proceedings* (2020), *33*(1), 13-22.

Ganesh Babu Loganathan, E. Mohan, R. Siva Kumar, Iot Based Water and Soil Quality Monitoring System. *International Journal of Mechanical Engineering and Technology (IJMET)* (2019), *10*(2), 537-541.

Suganthi K, Idris Hadi Salih, Ganesh Babu Loganathan, and Sundararaman K, A Single Switch Bipolar Triple Output Converter with Fuzzy Control. *International Journal of Advanced Science and Technology,* (2020), *29*(5), (2020), 2386 – 2400.

Ganesh Babu Loganathan, Can Based Automated Vehicle Security System. *International Journal of Mechanical Engineering and Technology (IJMET)* (2019), *10*(07), 46-51.

Loganathan, Ganesh Babu, Vanet Based Secured Accident Prevention System (2019). *International Journal of Mechanical Engineering and Technology, 10*(6), 2019, 285-291. https://ssrn.com/abstract=3451201

B.K. Patle, Ganesh Babu L, Anish Pandey, D.R.K. Parhi, A. Jagadeesh, A review: On path planning strategies for navigation of mobile robot, *Defence Technology, 15*(4), 2019, 582-606.

R. Sujith Kumar, G. Swaminathan, Ganesh Babu Loganathan, Design and analysis of composite belt for high rise elevators, *Materials Today: Proceedings, 22*(3), 2020, 663-672.

Dr.A.Senthil Kumar, Dr.Venmathi A R ,L.Ganesh Babu, Dr.G. Suresh, Smart Agriculture Robo With Leaf Diseases Detection Using IOT, *European Journal of Molecular & Clinical Medicine, 07*(09), 2462-2469.

Ganesh Babu L 2019 Influence of benzoyl chloride treatment on the tribological characteristics of Cyperus pangorei fibers based nonasbestos brake friction composites. *Mater. Res. Express* 7 015303.

Sivam, S.P.S.S., Loganathan, G.B., Kumaran, D., Saravanan, K., Rajendra Kumar, S., 2019. Performance Evaluation of Yield Function and Comparison of Yielding Characteristics of SS 304 in Annealed and Unannealed Conditions. *MSF* 969, 637–643.

https://doi.org/10.4028/www.scientific.net/msf.969.637

A. Devaraju, P. Sivasamy, Ganesh Babu Loganathan, Mechanical properties of polymer composites with ZnO nano-particle. *Materials Today: Proceedings* (2020), 22(3), 531-534.

Qaysar S. Mahdi, Prediction of Mobile Radio Wave Propagation in Complex Topography. *Eurasian Journal of Science & Engineering, 4*(1) (Special Issue); 2018, 49-55.

Qaysar S. Mahd, Survivability Analysis of GSM Network Systems. *Eurasian Journal of Science & Engineering, 3*(3), 2018, 113-123.

Qaysar S.Mahdi, Comparison Study of Multi-Beams Radar under Different Radar Cross Section and Different Transmitting Frequency. *Eurasian Journal of Science & Engineering, 3*(3); 2018, 1-11.

Ellappan Mohan, Arunachalam Rajesh, Gurram Sunitha, Reddy Madhavi Konduru, Janagaraj Avanija, Loganathan Ganesh Babu, A deep neural network learning-based speckle noise removal technique for enhancing the quality of synthetic-aperture radar images, *Concurrency and Computation-Practice & Experience,* https://doi.org/10.1002/cpe.6239.

Dr.A. Senthil Kumar, Dr.G. Suresh, Dr.S. Lekashri, L. Ganesh Babu, R. Manikandan, Smart Agriculture System with E – Carbage Using Iot, *International Journal of Modern Agriculture, 10*(1), 2021, 928-931.

Ganesh Babu Loganathan, Idris Hadi Salih, A.Karthikayen, N. Satheesh Kumar, Udayakumar Durairaj. (2021). EERP: Intelligent Cluster based Energy Enhanced Routing Protocol Design over Wireless Sensor Network Environment. *International Journal of Modern Agriculture, 10*(2), 1725 - 1736. http://www.modern-journals.com/index.php/ijma/article/view/908

C. Kannan, Nalin Kant Mohanty, R. Selvarasu, A new topology for cascaded H-bridge multilevel inverter with PI and Fuzzy control, *Energy Procedia, 117,* 2017, 917-926, https://doi.org/10.1016/j.egypro.2017.05.211

C. Kannan, and C.K. Kishore, A Comparision of Three Phase 27 Level Inverter Scheme under No Load and Multiple Load Conditions, *Bulletin of Electrical Engineering and Informatics,* 3(4), 245-250.

S. Priyadharsini, TS Sivakumaran, C Kannan, Performance analysis of photovoltaic-based SL-quasi Z source inverter *International Journal of Energy Technology and Policy,* 1(3), 254-264.

Maheswari, V., Nandagopal, V. and Kannan, C. (2016), Performance Metric of Z Source CHB Multilevel Inverter FED IM for Selective Harmonic Elimination and THD Reduction, *Circuits and Systems, 7,* 3794-3806. doi: 10.4236/cs.2016.711317.

Nandagopal, Dr.V., Maheswari, Dr.V. and Kannan, C. (2016) Newly Constructed Real Time ECG Monitoring System Using LabView. *Circuits and Systems, 7,* 4227-4235.

Qaysar Salih Mahdi, Idris Hadi Saleh, Ghani Hashim, Ganesh Babu Loganathan, Evaluation of Robot Professor Technology in Teaching and Business, *Information Technology in Industry,* 09(01), 1182-1194.

Dr.Mohammad, M. Othman. (2021). Properties of electron swarm parameters in Tetrahydrofuran. *International Journal of Modern Agriculture, 10*(2), 2412 - 2425. http://www.modern-journals.com/index.php/ijma/article/view/1036

Mohammad Mustafa Othman, Sherzad Aziz Taha, and Jwan Jalal Mohammad, Electron transport parameters in Hydrogen–argon mixtures, *AIP Conference Proceedings* (2017), 1888, 020040.

Dr.Mohammad M. Othman, Idris H. Salih, Sherzad A. Taha, Electron Transport Properties in Tetramethylsilane Vapour, *Solid State Technology* (2020), *63*(6), 10188-10200.

M. Othman, M., Taha, sherzad and Rasool Hussein, S. (2020) Boltzmann equation studies on electron swarm parameters for oxygen plasma by using electron collision cross – sections. *Zanco Journal of Pure and Applied Sciences, 32*(5), 36-53. doi: 10.21271/ZJPAS.32.5.4

Babu Loganathan, Ganesh; E. Mohan, Dr. High Quality Intelligent Database Driven Microcontroller Based Heartbeat Monitoring System. *International Journal of Engineering & Technology,* [S.l.], 7(4.6), 472-476, 2018. ISSN 2227-524X.

Othman, M., Taha, S. and Salih, I. (2019) Analysis of Electron Transport Coefficients in SiH4 Gas Using Boltzmann Equation in the Presence of Applied Electric Field. *Zanco Journal of Pure and Applied Sciences, 31*(1), 77-88. doi: 10.21271/zjpas.31.1.10.

Muthuramalingam, T., Saravanakumar, D., Babu, L.G. 2020. Experimental Investigation of White Layer Thickness on EDM Processed Silicon Steel Using ANFIS Approach. *Silicon 12,* 1905–1911. https://doi.org/10.1007/s12633-019-00287-2

G, Sai Krishnan and Loganathan, Ganesh Babu and K, Selva Ganapathy and N, Srivathsan and M, Vasanth and G, Venkatateja, Development of Superhydrophobic Nanocomposite Coatings on FRP Sheet Surface for Anti-Icing and Wear-Resistance Applications (2019). *Proceedings of International Conference on Recent Trends in Computing, Communication & Networking Technologies (ICRTCCNT)* 2019.

https://ssrn.com/abstract=3432305 or http://dx.doi.org/10.2139/ssrn.3432305

S.P. Sundar Singh Sivam, Ganesh Babu Loganathan, K. Saravanan, S. Rajendra Kumar. (2019). Outcome of the Coating Thickness on the Tool Act and Process Parameters When Dry Turning Ti–6Al–4V Alloy: GRA Taguchi & ANOVA. *International Journal of Innovative Technology and Exploring Engineering (IJITEE)*, 8(4), 419-423.

Sivam Sundarlingam Paramasivam, S., Loganathan, G., Kumaran, D., Saravanan, K. et al., *Function of Taguchi Grey Relation Analysis for Influencing the Process Parameter for Getting Better Product Quality and Minimize the Industrial Pollution by Coolants in Turning of Ti-6Al-4V Alloy,* SAE Technical Paper 2019-28-0065, 2019, https://doi.org/10.4271/2019-28-0065

Sivam S.P.S.S., Loganathan G.B., Saravanan K., Dinesh Guhan S., Banerjee A. (2021) *Effects of Drilling Process Parameters Using ANOVA and Graphical Methods.* In: Kumaresan G., Shanmugam N.S., Dhinakaran V. (eds) Advances in Materials Research. Springer Proceedings in Materials, 5. Springer, Singapore.

https://doi.org/10.1007/978-981-15-8319-3_35

Muthuramalingam T., Ganesh Babu L., Sridharan K., Geethapriyan T., Srinivasan K.P. (2020).

Multi-response Optimization of WEDM Process Parameters of Inconel 718 Alloy Using TGRA Method. In: Sattler KU., Nguyen D., Vu N., Tien Long B., Puta H. (eds) Advances in Engineering Research and Application. ICERA 2019. Lecture Notes in Networks and Systems, vol 104. Springer, Cham.

https://doi.org/10.1007/978-3-030-37497-6_56

Babu, L.G. (2020). Influence on the Tribological Performance of the Pure Synthetic Hydrated Calcium Silicate with Cellulose Fiber. *In Journal of the Balkan Tribological Association, 26*(4), 747–754.

Sai Krishnan G., Shanmugasundar, Pradhan R., Loganathan G.B. (2020) *Investigation on Mechanical Properties of Chemically Treated Banana and Areca Fiber Reinforced Polypropylene Composites.* In: Praveen Kumar A., Dirgantara T., Krishna P.V. (eds) Advances in Lightweight Materials and Structures. Springer Proceedings in Materials, 8. Springer, Singapore. https://doi.org/10.1007/978-981-15-7827-4_27

Dr. Othman, M.M., Ishwarya, K.R., Ganesan, M. and Babu Loganathan, G. (2021). A Study on Data Analysis and Electronic Application for the Growth of Smart Farming. *Alinteri Journal of Agriculture Sciences, 36*(1): 209-218.
doi: 10.47059/alinteri/V36I1/AJAS21031